scientific reports

Check for updates

OPEN

New nanomanufacturing strategy through bioinspired design, for promising treatment of Parkinson's disease

Aliaa A. Razzak[1,2], Zahraa S. Al-Garawi[1]✉, Adawiya J. Haider[3] & F. A. A. N Bahaa Hassan[4]

This study attempts to develop a new nanomanufacturing strategy for Parkinson's disease using natural biodegradable components (chitosan, albumin, and dopamine) that can penetrate the blood-brain barrier (BBB) due to biocompatibility, biodegradability, targeted delivery, and controlled drug release. It was prepared, thoroughly optimized and characterized using various biophysical and chemical techniques. Results showed that the nanomanufactured system (molar ratio of 1:0.25:0.5 and particle size range: 38–190 nm) exhibited a zeta potential of + 73 mV facilitating efficient pentration of BBB through an adsorption mechanism with the cell membrane's negative charges. The particle size of the nanomanufactured system and spherical nanoparticle clusters indicated its ability to enhance dopamine delivery to brain tissues. Encapsulation efficiency was measured at 74.31 ± 0.29 with dopamine release faster at pH 5.4 and sustained release over 96 h in both acidic media (pH 5.4) or physiological conditions (pH 7.4). Cytotoxicity studies showed a degradation rate in normal cells that never exceeded 20% and the nanomanufactured system exhibited low half-maximal inhibitory concentration (IC50) values, indicating low cytotoxicity. Albumin plays a vital and distinct role in stimulating normal cells and enhancing the transport system to the target via an adsorptive–mediated endocytosis pathway. The electron microscopy images depict distrution of heterogeneous nanoparticles, with sizes ranged from 36.86 nm to 190.3 nm and a mean average diameter of 108.1 nm. The average particle size of the nanosystem was 49.4 ± 9.9 nm, with a Polydispersity Index (PI) of 0.494. The loading efficiency was 14.78 ± 0.37% and the encapsulation efficiency was 74.31 ± 0.29%. This nanomanufactured system holds significant promise for improving Parkinson's disease treatment by enabling targeted and efficient drug delivery to the brain.

Keywords Parkinson's disease, Dopamine hormone, Albumin, ROS scavenge, Mediated adsorptive endocytosis, Cytotoxicity

Parkinson's disease (PD), a complex and progressive neurodegenerative disorder, is pathologically characterized by the loss of nigrostriatal dopaminergic neurons. This loss leads to the hallmark symptoms of PD: bradykinesia, resting tremor, and rigidity[1–4]. The degeneration of these neurons in the substantia nigra pars compacta, accompanied by the reduction of dopamine, is a key pathological feature of PD[5,6]. Intracellular aggregates of α-synuclein, forming Lewy bodies and Lewy neurites, are also significant markers of the disease[1].

Over two centuries since James Parkinson's description of "shaking palsy," the global prevalence of PD continues to rise, affecting approximately 7–10 million people worldwide. By 2040, projections indicate that this number will rise to 12.9 million[3]. In Iraq, according to the latest WHO announcement in 2020, PD deaths were 658 or 0.45% of the total deaths. The age-adjusted death rate was 4.74 per 100,000 of the population ranking Iraq #59 in the world. The number of incidents from 2010 to 2023 moved from 177.5 ± 3.54 to 197.5 ± 24.75. However, the occurrences of PD according to gender, as consulting in the center of PD in Iraq, *Saad ELwitry*, Fig. 1.

Recent advancements in nanomedicine have explored the use of polymeric and lipid nanoparticles for dopamine and levodopa delivery to the brain[1,2,8]. However, Levodopa, the primary treatment of PD, has

[1]Chemistry Department, Collage of Science, Mustansiriyah University, Baghdad, Iraq. [2]Applied Sciences Department, Chemistry Branch, University of Technology, Baghdad, Iraq. [3]Applied Sciences Department, Laser Science and Technology Branch, University of Technology, Baghdad, Iraq. [4]Department of Neurology, Sàad Al-Wittry neuroscience hospital, Baghdad, Iraq. ✉email: z.mohsin@uomustansiriyah.edu.iq

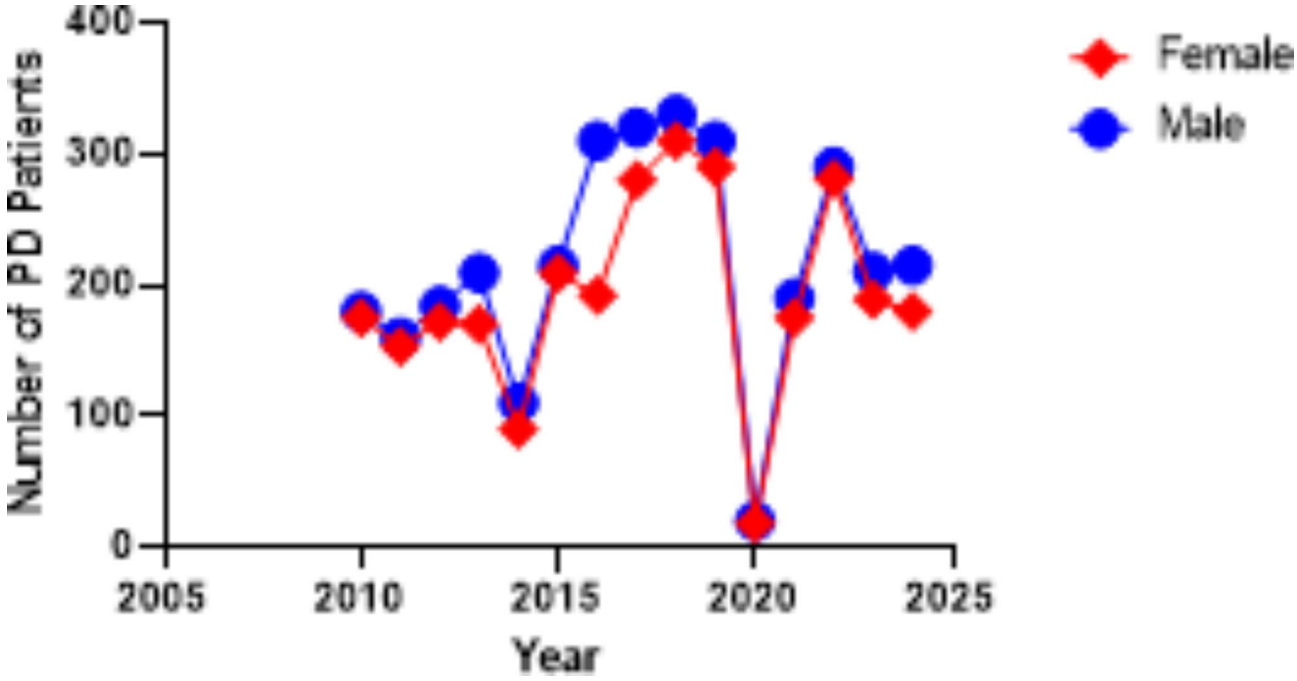

Fig. 1. Number of PD patients between (2010 to 2024) for movement disorder consulting in the center of PD in Iraq *Saad ELwitry*.

limitations, including a short half-life and potential severe dyskinesia. Studies utilizing albumin/poly (lactic-co-glycolic acid) (PLGA) nanoparticles conjugated with dopamine have successfully crossed the BBB[1]. Because dopamine is a critical neurotransmitter in the brain, it plays a pivotal role in regulating movement, mood, and motivation. It is synthesized in specific brain regions[7–10]and converted into norepinephrine and epinephrine[5]. Dopamine also exhibits antioxidant properties, protecting neurocytes from oxidative stress and scavenging free radicals[1]. Oxidative stress closely links its metabolism to dopamine, thereby contributing to dopaminergic neurotoxicity. The impairment of dopaminergic neurotransmission in PD may exacerbate corticostriatal glutamatergic transmission, contributing to the imbalance in basal ganglia's functional output[11–14]. Nanoparticles offer a promising approach to overcome these challenges and enable drug delivery across the BBB[15–18]. On the other hand, medical applications using bovine serum albumin (BSA)-based nanoparticles have been explored, including PD[3,19]. BSA, has multiple ligand binding sites and a long circulatory half-life, making it an ideal candidate for drug delivery systems. Its ability to permeate the BBB via receptor-mediated pathways is crucial for effective brain-targeted drug delivery. In addition, chitosan, a biocompatible and biodegradable natural polymer, has shown potential in drug delivery systems, particularly for targeting the brain[20–23]. Chitosan's positive charges enhance the permeation of drugs across cell membranes, facilitating drug transport[16,24].

Therefore, we aimed here to show the potential of a novel nanomanufactured system of chitosan-albumin-dopamine [Cs-Alb-Dop] to effectively penetrate the BBB due to some advantages such as biocompatibility, biodegradability, targeted delivery, and controlled drug release. We here focus on the preparation, characterization, biocompatibility, toxicity, and stability of this system, thereby providing a promising therapeutic approach for PD.

Materials and methods

Reagents

Dopamine hydrochloride was obtained from Sigma-Aldrich (St. Louis, MO, 63103 USA) and stored in a dry place, ideally at temperatures ranging from 2 to 8 °C. Nano Chitosan, with a particle size exceeding 80 nm, low molecular weight, and 95.7% purity, was supplied by Sang Herb Company, China. Phosphate buffer saline (PBS) was procured from BDH, England. Unless otherwise specified, we purchased all other reagents from Sigma-Aldrich (St. Louis, MO, USA). The preparation process was conducted at room temperature (RT) using double deionized water (DDW) of 99.99% purity.

Preparation of the nanosystem [CS-Alb-Dop]

The nanosystem was prepared based on previous methods[5,9,25] with modification. The modified method included the preparation of 2 parts solutions. **A**. Preparation of nano hitosan: 4.5 g of nano chitosan was dissolved in 150 ml of 1% acetic acid, followed by low-frequency ultra-sonication (Ultrasonic Cell disrupter, UCD-150, P/V150W/220V50Hz, biobased, Shandong, China, CO, LTD) for 2 min. **B**. Albumin solution: 1.12 g of albumin was added to 100 ml of phosphate buffer saline PBS (1 g of albumin per 100 ml of PBS). The mixture of A and B was stirred at 1500 rpm at room temperature under an argon gas atmosphere. After 2 min of sonication and

continuous magnetic stirring at 1500 rpm, the mixture was maintained in a water bath at 40 °C. Subsequently, 2.25 g of dopamine was dissolved in 50 ml of distilled water (DIO). This mixture was then left to stir on a hot plate for 30 min. Finally, a supersaturated solution of TPP (in 25 ml of distilled water) was added to the mixture. The drug was isolated using a cooling centrifuge (Sigma 3-16KL, Germany) at 11,500 rpm and room temperature for 30 min. This centrifugation step was repeated thrice to achieve enhanced washing in DIO. The resulting product formed a gel, preserved at -8 °C, and could be transformed into a powder post-drying.

Characterization of nano-manufactured system [CS-Alb-dop

Characterization of the manufactured nanosystem was performed using many techniques, such as: SEM, AFM, FTIR, XRD, zeta potential, and cytotoxicity.

Scanning Electron Microscopy (SEM)

The morphology of the nanomanufactured system was studied using a LEO 1525 field emission scanning electron microscope FESEM (Zeiss, Oberkochen, Germany). Samples were placed on aluminum stubs with double-sided conducting carbon tapes and coated with a 50/50 Au/Pd mixture, scanned at 25 kV. Additional microscopy was performed using an Axichemi Sem Thermo Scientific Company, Holland.

Atomic Force Microscopy (AFM)

The morphology of the nanomanufactured system and its components were determined using AFM (Dimension Icon, Bruker, USA). A drop of the nano system solution (1 mg/ml) was placed on freshly cleaved mica. After 3 min of incubation, the surface was gently washed with deionized distilled water to remove unbound nanoparticles.

Fourier Transform Infrared (FTIR) Spectroscopy

The composition of the nanomanufactured system was analyzed using a Nicolet 6700 infrared detector (Thermo Fisher Scientific, USA). The sample, along with KBr, was pressed into pellets at a pressure of 300 kg/cm^2. FTIR spectra were obtained by averaging 32 interferograms within the 1000–4000 cm^{-1} range at a resolution of 2 cm^{-1}.

UV–Vis spectroscopy

The optical absorption was measured using a double beam UV–Vis spectrophotometer (Aquarius 7000) within a range 200–800 nm. Spectra were recorded between 200 and 800 nm using Shimadzu UV-1800 double-beam UV-Vis transmittance spectrophotometer (Japan) with a scanning range of 200 to 1200 nm.

X-ray diffraction (XRD)

The crystal structures of the nanomanufactured system and its components were examined using a RIGAKU X-ray diffractometer (model Minifex IL, USA), utilizing CuKα radiation. We conducted measurements at 30 kV and 25 mA, scanning a range of 5°–65° at an interval of 1°/min.

Particle size and zeta potential measurements

The zeta potential of the nanomanufactured system and its components was measured using a Zetasizer Nano-ZS (Malvern Instruments, UK). After preparing a 1 mg/ml nanoparticle drug solution in double distilled water, the mixture was sonicated for 15 s in an ice-cold bath. Measurements were performed at room temperature using three independent replicates.

Standard curves

Standardization of dopamine Fig. 2a and b were recorded using a calibration curve that was prepared by recording dopamine spectra solutions via absorbance at 280 nm and plotting against the known dopamine concentrations. The values points were fitted with a linear regression equal to 0.9948. The unknown concentration of dopamine was calculated by inserting the measured.

Protein concentration by Bradford Test at 595 nm

A volume of 500 µL of the sample was initially taken. To this, 450 µL of PB was added, ensuring the dilution and proper dispersion of the sample within the buffer solution. Following this, a significant volume of 2500 µL of Comasic Blue reagent was introduced to the mixture. Comasic Blue, known for its ability to bind protein molecules, thus allowing for the quantification of protein concentration through absorbance measurement, was crucial for this assay. Upon the addition of all components, the mixture was thoroughly mixed to ensure uniformity. It was then left to stand for a period of 2 min. This waiting time is necessary for the reaction between Comasic Blue and the proteins in the sample to finish. This makes it possible for a color change to happen which shows how concentrated the proteins are.

Control preparation [Blank]

For the preparation of the control (blank) solution, a foundational step in ensuring the accuracy of spectrophotometric measurements, a precise volume of 50 µL of PB was first prepared. This buffer serves as the solvent base, providing a consistent medium for the subsequent addition of reagents. Following this, 2500 µL of Comasic Blue reagent were added to the phosphate buffer. Comasic Blue, a dye renowned for its protein-binding capabilities, is essential in this context for establishing a baseline absorbance level in the absence of the sample's protein. The spectrophotometric analysis relies on this blank solution to calibrate the instrument and attribute any measured absorbance to the sample, not background interference. By carefully mixing these two parts without the protein sample present, it is possible to accurately find out how much protein is in later samples by comparing them to this blank baseline.

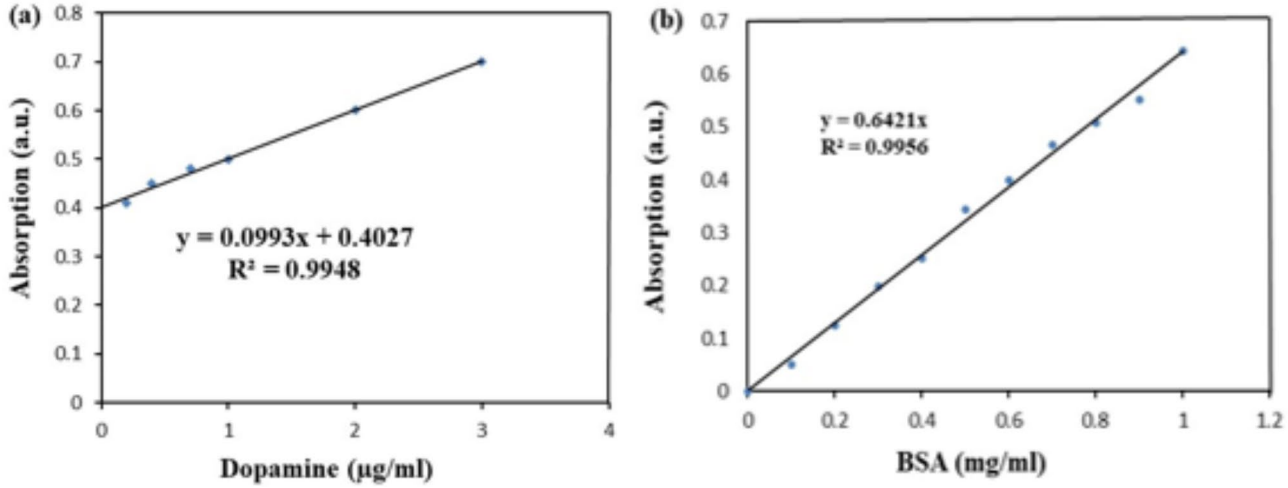

Fig. 2. Standard curve of dopamine (a), and BSA (b).

Encapsulation and loading efficiency

A weight of 5 mg of [Cs-Alb-dop] was dispersed in 50 ml of PBS under sonication, centrifuged at 15,000 rpm for 1 h, and the supernatant was collected. The concentration of dopamine in the supernatant was measured at 280 nm using a nano drop (Nano Drop™ 2000/2000c spectrophotometers, Thermo Fisher Scientific, Boston, USA). The encapsulation efficiency and the loading content of [Cs-Alb-Dop]were calculated using the following formulas[9]:

$$\text{Encapsulation efficiency } (\%) = \frac{mass\ of\ the\ drug\ in\ nano\ particals}{mass\ of\ the\ drug\ used\ in\ formulation} \times 100\% \quad (1)$$

$$\text{Drug loading efficiency } (\%) = \frac{Amount\ of\ drug\ loaded}{Total\ weight\ of\ carrier\ system} \times 100\% \quad (2)$$

Dopamine release

The release of dopamine from the nanomanufactured system was thoroughly investigated using a nano drop (Nano Drop™ 2000/2000c Spectrophotometers, Thermo Fisher Scientific, Boston, USA). The nanosystem was placed in two (6 cm) dialysis bags (MWCO 1000 Da), one immersed in 100 mL of citrate buffer (pH 5.4), and the other in 100 mL of PB (pH 7.4). Both solutions were maintained under constant stirring. At time intervals, 0, 4, 8, 12, 24, 48, 72, and 96 h, 2 mL samples were carefully withdrawn from each 100 mL buffer solution and immediately replaced with an equal volume of fresh buffer with the corresponding pH. A volume of 2 mL buffer was withdrawn from each interval and used to determine the free unbound protein. The concentration of dopamine released into the buffer solution was estimated.

Cytotoxicity assay (MTT)

This test was carried out through the following steps:

Collection of white blood cells (Lymphocytes)

A blood sample was obtained from a healthy male volunteer, aged 25 years, under highly sterile conditions. A total of 10 mL of venous blood was collected in the anticoagulant tube and centrifuged at 5000 rpm for 5 min. The buffy coat layer of the supernatant, rich in white blood cells, was carefully collected using a sterile glass Pasteur pipette. These cells were then transferred to a laboratory tube containing 5 mL of sterile RPMI-1640 medium, supplemented with 10% fetal calf serum (FCS). This procedure ensured a final concentration of 1×10^4 white blood cells per mL, preparing them for subsequent cytotoxicity.

Viability of lymphocytes

Prior to conducting the cytotoxicity assay, it was crucial to confirm the viability of the isolated lymphocytes. This was achieved by mixing equal volumes (100 µl each) of WBC suspension and 1% Trypan blue. The mixture was then incubated for 3 min at 37 °C. Post-incubation, the cells were examined under a light microscope at 40X magnification. Both pigmented and non-pigmented cells were counted on a hemocytometer. For the cytotoxicity test to be valid, the viability of the lymphocytes needed to be at least 98%.

Cell seeding

To investigate the cytotoxic effects on WBC, higher concentrations of albumin, chitosan, dopamine, the nano mixture, and the final mixture were prepared in PBS, pH 7.2 ± 0.2. Concentrations of 0.0, 1, 5, 10, 15, 20, 25, 50, and 100 µg/mL were obtained using Roswell Park Memorial Institute (RPMI) medium. The experiment was conducted in 96-well microtiter plates. A suspension of WBC, containing 1×10^4 cells/mL, was transferred into

each well of the 96-well plate, which was gently swirled in a circular motion to ensure thorough mixing of the cell suspension with the nanoparticles. The plates were then covered and incubated at 37 °C for 24 h. In the day after, the plates were again swirled gently for 3–4 min to dislodge non-adherent cells. The excess medium was then removed and discarded. Column number 1 in each plate was designated as the negative control.

Concentration optimization
A series of concentrations of the nanomanufactured system was prepared in a tissue culture medium devoid of fetal calf serum. These were added to wells containing adherent WBC. Each treatment was replicated three times. The culture medium was added to the tissue culture plates, with Column No. 1 serving as the negative control, to which 200 µL of serum-free culture medium was added. Columns 2 to 12 received gradient concentrations of 200 µL per well. The plates were then covered and incubated at 37 °C for varying exposure times (24–28 h).

Cytotoxicity assay
After the designated incubation period, the contents of the plates were discarded, and the wells were washed three times with PBS to remove any residual material and non-adherent cells. Subsequently, 10 µL of MTT dye solution (final concentration of 0.5 mg/mL) were added to each well and incubated for 4 h at 37 °C in a carbon dioxide incubator. The cells were washed several times with PBS until all excess dye was removed. Once the plates were completely dry, 100 µL of DMSO were added to each well to ensure complete dissolution of the violet granules. The results were read using an ELISA microplate spectrophotometer at a wavelength of 500 nm. The inhibition rate (IR) was calculated using Eq. (4):

$$IR = \frac{A - B}{A} \times 100\% \tag{3}$$

Where: IR is the inhibitory rate,
A is absorbency for negative control,
and B is absorbency for the test.

Hemocompatibility Test
A blood compatibility test was conducted at various concentrations (0, 1, 5, 10, 15, 20 µg/mL). Blood was drawn intravenously from a healthy 35-year-old individual and placed in test tubes containing EDTA as an anticoagulant. A mixture of 0.5 mL of whole blood with 4.5 ml of normal saline solution was prepared, serving as the negative control. The positive control tube contained deionized distilled water (DDW) to induce 100% hemolysis. All tubes were incubated at 37 °C for one hour, followed by centrifugation at 3000 rpm for 5 min. The absorbance was measured using a UV-Vis spectrophotometer at 540 nm. The hemolysis rate was determined using the following Eq. (5):

$$\text{Hemolysis}\% = \frac{(\text{Ab specimen} - \text{Ab control } (-\text{ve}))}{(\text{Ab control } (+\text{ve}) - \text{Ab control } (-\text{ve}))} \times 100$$

Ethical approval
On 2/1/2023, the College of Science registered and approved this project under registration no. P.G. 5. It has been considered by the scientific and ethical committee at Mustansiriyah University. It meets the requirements of the Helsinki Declaration.

Results and discussion

Scanning Electron Microscopy (SEM)

SEM was employed to investigate the morphology and size of [Cs-Alb-Dop]. The pure nano chitosan exhibited distinct surface characteristics compared to the system Fig. 2. Due to its large molecular structure, dopamine presents a variety of morphological shapes, including spherical and rectangular ones. Figure 3showed SEM images of nanomanufactured systems revealing a smooth crystal-like morphology, a characteristic that could be pivotal in enhancing the system's interaction with biological environments. The uniformity and smoothness of the crystals suggest a controlled and consistent synthesis process. The images depict a heterogeneous size distribution of the nanoparticles, with sizes ranging from 36.86 nm to 190.3 nm. The formation of spherical particle clusters, indicated the nanomanufactured's self-assembly properties. These spherical clusters can provide a high surface area-to-volume ratio, which is beneficial for drug loading and release. The spherical shape is also known to be favorable for biocompatibility and reduced cytotoxicity, making the nano-manufactured potentially safer for in vivo applications. These characteristics are crucial for its intended use in biomedical applications, particularly in targeted drug delivery, where size, shape, and surface properties play a significant role in the system's performance and interaction with biological tissue[25,26].

Atomic force microscopy

Topographical maps of the surface revealled the albumin surface`s spherical roughness, Fig. 4. The highest molecular structures, as observed in both 3D shapes and Table 1., showed a height of 96.1 nm, with a mean average diameter of 116 nm. The histogram of size distribution for albumin indicated a range between 10 and 60 nm in mean height. In contrast, dopamine has a shorter height of 11.9 nm, a rough surface, and a mean height of 47.29 nm. The nano-manufactured [Cs-Alb-Dop] displayed a notably smoother surface compared to its components. It features higher atomic structures, with a mean height of 40 nm. This nano-manufactured material's size distribution histogram showed a mean height of 37.86 nm and a mean average diameter of

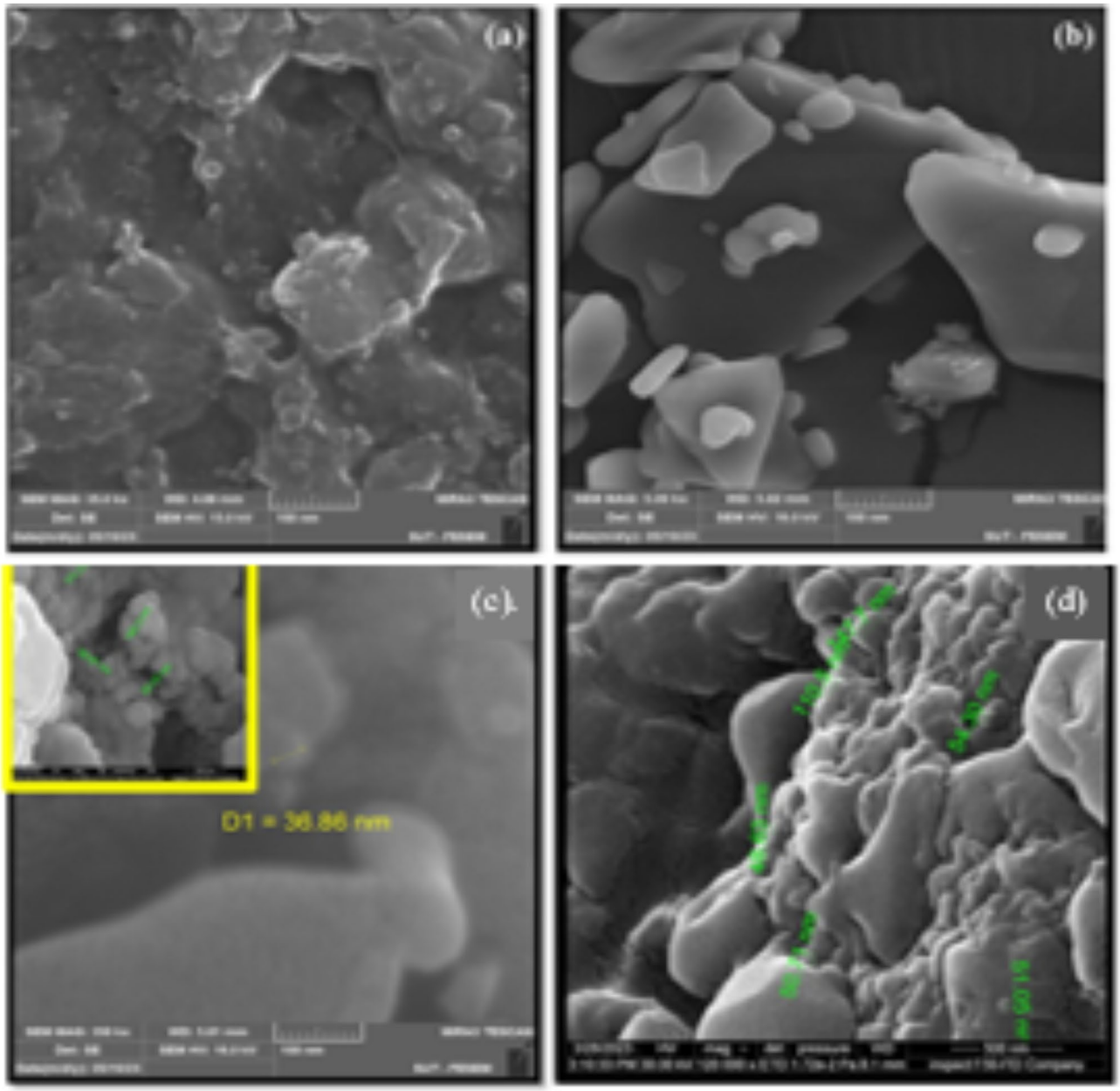

Fig. 3. Scanning Electron Microscopy images of nanochitosan (**a**) and dopamine (**b**), nanomanufactured system [Cs-Alb-Dop] (**c**) and (**d**).

108.1 nm. This suggests a narrow size distribution of particles within the nanoscale range. The smoother surface of the nanomanufactured, compared to the rougher surfaces of its individual components, suggests better biocompatibility and possibly enhanced interaction with biological membranes. The narrow size distribution, particularly with the smaller mean diameter, is crucial for uniformity in drug delivery applications. Smaller nanoparticles are often preferred for their ability to penetrate biological barriers more effectively, making them ideal for targeted drug delivery systems such as those intended for crossing the blood-brain barrier in PD treatment[9] see Fig. 3.

X-ray diffraction measurement (XRD)

Figure S1 in the supplementary results shows the crystallinity of the [Cs-Alb-Dop]. The XRD pattern of albumin protein and nano-manufactured exhibited a broad peak, indicative of its amorphous nature. Dopamine showed multiple peaks, characteristic of bulk molecules containing large units or groups. The prepared [Cs-Alb-Dop] was analyzed in deionized water see figure S1 in supplementary results. The XRD diffraction patterns did not reveal any impurity peaks, indicating that the nanoparticles produced were pure and crystalline. The drug system demonstrated high periodicity. Chitosan and albumin were amorphous structures. Dopamine exhibited more

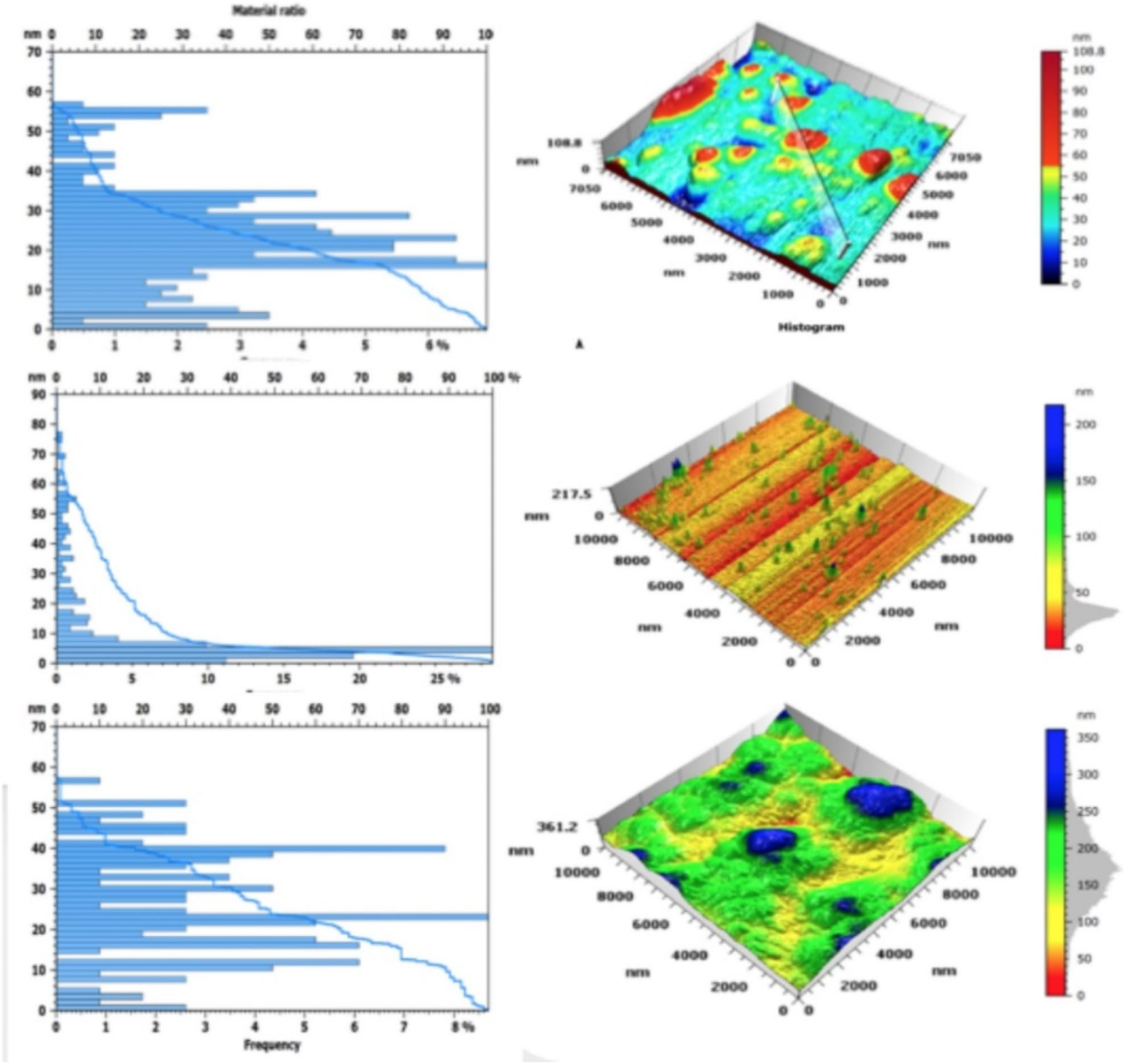

Fig. 4. AFM topography images of albumin (A), dopamine (B) and nano-manufactured (C).

Drug and components	Mean average diameter (nm)	Height distribution (nm)	Mean height (nm)
Albumin (BSA)	116	96.1	36.39
Dopamine(DOP)	105.7	11.9	47.29
Nanomanufactured [Cs-Alb-Dop].	108.1	40	37.86

Table 1.. Summarized topography information of the results of nanosystem.

peaks due to its larger molecular structure. In the nano-manufactured, the most prominent peak was observed at 27°A, significantly higher than the residual peaks. This high diffraction and purity peak at 27 °A confirmed the formation of [Cs-Alb-Dop]. At this peak, the particle size was calculated to be 76.974 nm using the Scherrer Eq. 4, a method employed for determining particle size.

$$\tau = \frac{\kappa \lambda}{\beta \cos\vartheta} \tag{4}$$

FTIR analysis

The FTIR spectrum of dopamine at 400–4000 cm^{-1}, revealed characteristic primary amine bending and stretching modes at 1616 cm^{-1} and 1500 cm^{-1}. Additionally, peaks at 3232.70 cm^{-1} and 3055.24 cm^{-1} represented the stretching vibrations of catechol-OH, indicative of intramolecular hydrogen bonds. The peak around 2954.95 cm^{-1} corresponded to the stretching vibrations of C-H. The strong and overlapping peaks between 1616.35 cm^{-1} and 1500.62 cm^{-1} were attributed to the bending of N-H in the primary amine group of the neurotransmitter and the stretching vibrations of C-C in aromatic rings. The FTIR spectrum of chitosan displayed characteristic peaks, including -NH and -OH group stretching at 3435 cm^{1}, -CH stretching at 2920 cm^{1}, and the C = O stretching of amide I and II bands. These findings are crucial for understanding the molecular structure and interactions within the nanosystem [Cs-Alb-Dop].

BSA contains two tryptophan residues, Trp 134 and Trp 212, located on the molecule's surface and within a hydrophobic pocket. This structural arrangement enhances the affinity of polyphenols for BSA, leading to protein unfolding and the relocation of amine groups, thiol groups, and hydrophobic regions to the molecule's surface. This lead to increase intramolecular binding and a reduction in hydrophobic interactions. The amide I band is widely used to quantify the secondary structure and conformational changes of proteins and polypeptides, is particularly useful for studying protein misfolding and aggregation[9]. The secondary structures of BSA include α-helix, β-sheet, β-turn, and random coil.

Table S1and Fig S2 show the functional groups in the nanomanufactured system. Some shifting in the groups indicated alterations in the secondary structure of the protein within the nano-manufactured [Cs-Alb-Dop]. The FTIR spectra of Cs-Alb Dop revealed two sharp signals at 1654.92 cm^{-1} and 1539.20 cm^{-1} and a weak signal at 1381.03 cm^{-1}, corresponding to the peptide bonds in the protein. The ester appeared at 1735.39 cm^{-1}, and alkane C-H at 2858.51 cm^{-1}, indicating N-H and C-H alkane stretching. The hydrogen bonding was detected at 3417.86 cm^{-1}, suggesting N-H and C-H alkane stretching. Fig S2 indicated that the final result (nano-manufactured) shifting in O-H bands, N-H, and C = O due to hydrogen bonding which changed the intensity of the absorption band it became more intense and broad in the hydrogen bonding, and the N-H bond in the amide group. The result confirmed the successful interaction between nano chitosan and albumin with dopamine by conjugation of the amine side of chitosan and the carboxyl side of amino acid in the BSA via amide information. The abundance of nanochitosan, means more amine sides in the system that increases the ability of interact the amine sides with hydroxyl sides in dopamine and with amine group in the other side by using TTP as binding agent then forming a positive charge and facilitating the penetration BBB through the absorptive endocytosis adsorption[27–32].

UV spectroscopy

Analysis of the UV spectrum of the nanomanufactured system, significates insights into the molecular interactions and structural changes induced upon the formation of the nanocomposite. Fig S3 showed that absorption peaks within the 200–400 nm range, specifically at 210 nm and 278 nm, are traditionally associated with the intrinsic electronic transitions of proteins and aromatic amino acids, respectively. Notably, the presence of tryptophan residues, Trp 134 and Trp 212, in bovine serum albumin (BSA) plays a crucial role in the observed spectral characteristics, where these residues are known for their potential to undergo $\pi \rightarrow \pi^*$ and $n \rightarrow \pi^*$ transitions.

Upon integration into the nano-manufactured system, a noticeable blue shift in the absorption bands at 196, 280, and 344 nm was observed, compared to the spectrum of dopamine alone. This shift suggests a reconfiguration of the electronic environment surrounding the tryptophan residues and the dopamine molecules, indicative of $n \rightarrow \pi^*$transitions. The formation of the nanomanufactured system seemingly constrains these molecules within a more rigid structural framework, thereby increasing the energy required for electronic transitions. This phenomenon not only highlights the complex intermolecular interactions within the nanomanufactured system but also underscores the altered electronic and chemical properties resulting from the nanocomposite formation.

The enhanced interaction between chitosan and albumin, facilitated by the incorporation of dopamine, is reflected in the increased intensity and the blue shift of the absorption bands. Such changes are emblematic of conformational and chemical modifications within BSA, likely as a result of its interaction with the other nanomanufactured system components. These modifications affect the non-bonding electrons' energy levels, particularly those involved in $n \rightarrow \pi^*$transitions, thereby altering the UV-visible absorption characteristics. The observed spectral shifts and intensity changes are thus a testament to the dynamic electronic interactions at play, shedding light on the potential of the Cs-Alp-Dop nanosystem for targeting drug delivery applications, especially in traversing biological barriers such as the BBB. This analysis not only provides a deeper understanding of the nanosystem's structural and electronic configuration but also opens avenues for further exploration of its biomedical applications see Fig S3 in supplementary results[27–30].

Particle size [Cs-Alb-dop]

The average particle size of this nanomanufactured system was 49.4 ± 9.9 nm, with a Polydispersity Index (PI) of 0.494. This finding confirmed that the particle size of nano system falls well within the nanoscale range, specifically below 200 nm, which is essential for its effectiveness in biomedical applications, see Figure S4 in the supplementary.

Zeta potential

The zeta potential (ζ) of nano chitosan was measured at 66.7 mV, indicating a high level of stability. In contrast, the ζ-potential for albumin was – 0.9 mV at 25 °C, and for dopamine was – 1.3 mV. These values reflect the surface charge of each component in the nanosystem. The ζ of nanomanufactured system was 73 mV, which referred to

the stability and the potential to penetrate the BBB through adsorptive-mediated endocytosis. At a pH lower than 6.5, the amine groups in chitosan are protonated, making the polymer soluble in most organic acids. However, at a pH higher than 6.5, chitosan becomes insoluble due to the deprotonation of these amine groups. This pH-dependent solubility is crucial for the targeted delivery and release of the drug within specific physiological environments. The use of dopamine-conjugated BSA nanoparticles in drug delivery offers several advantages, including targeted delivery, biocompatibility, controlled release kinetics, stability, and multifunctionality[31,32]. Accordingly, as we aimed to treat PD, the positive charge of our nanosystem should facilitate the delivery of anti-neuroexcitation peptides to brain cells through adsorption-mediated transcytosis. see Fig. 5.

In general, ζ-potential values exceeding 30 mV refer to good stability of the nanoparticles, while values above 60 mV indicate excellent stability. A value of 20 mV suggests short-term stability, whereas values ranging between −5 mV and 5 mV indicate rapid aggregation. Many researchers prefer cationic nanotherapy due to its efficiency, safety, and ease of use in carrying therapeutic substances. The particle size analysis of the nano-system [Cs-Alb-Dop] is crucial for understanding its behavior in biological systems. Particle size can influence the system's distribution, cellular uptake, and overall therapeutic efficacy. The analysis provides insights into the uniformity and range of particle sizes within the nano-system, which are essential parameters for ensuring consistent drug delivery and performance.

Encapsulation efficiency

The calculated encapsulation efficiency was 74.31 ± 0.29%, and the drug loading efficiency was 14.78 ± 0.37%. The analysis revealed that the amount of free, unloaded dopamine was 0.2569 mg, the amount of drug loaded was 0.7431 mg and the total weight of the carrier system was 5 mg[32,33].

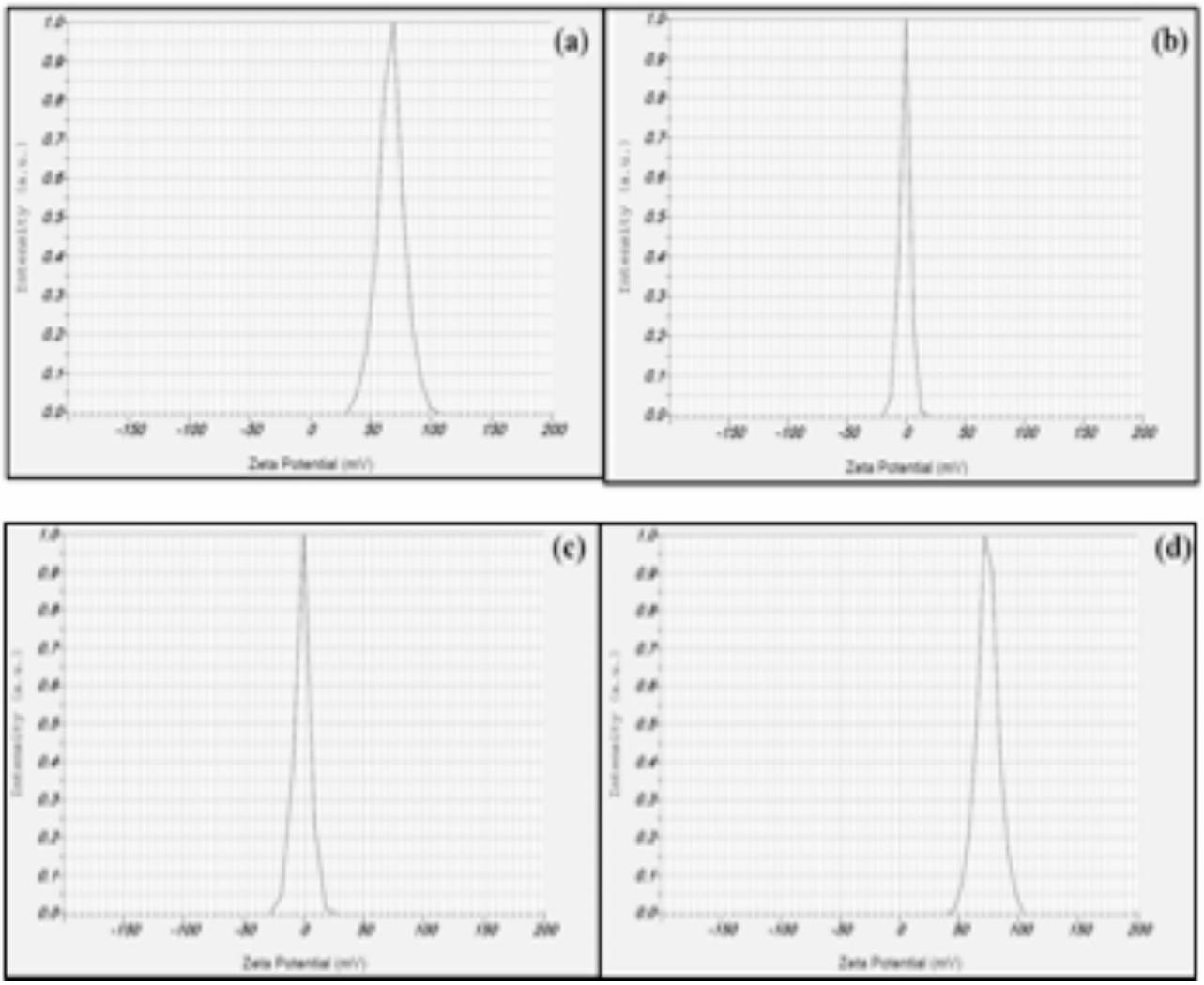

Fig. 5. Zeta Potential of nano chitosan (Nano Cs) (a), BSA (b), dopamine (c), and nanosystem [Cs-Alp-Dop] (d).

Dopamine release

The release profile of dopamine from the nanocomposite was thoroughly investigated using Nanodrop (NanoDrop™ 2000/2000c Spectrophotometers, Thermo Fisher Scientific, Boston, USA). The [Cs-Alb-Dop] was encapsulated in two 6 cm dialysis bags (MWCO 1000 Da) and each was immersed in separate beakers. One beaker contained 100 mL of citrate buffer (pH 5.4) and the other 100 mL of phosphate buffer (pH 7.4), both under constant stirring. At specific time intervals (0, 4, 8, 12, 24, 48, 72, and 96 h), 2 mL samples were extracted and immediately replaced with fresh buffer. The dopamine concentration in these samples was measured, establishing a correlation between absorption maxima at 280 nm and dopamine concentration. This analysis, depicted in Fig. 6, provided insights into the release kinetics and cumulative release percentage of dopamine from the nanocomposite, crucial for understanding the controlled release behavior of the system.

In vitro studies: cytotoxicity assay (MTT assay)

The cytotoxicity of the nano-manufactured system [Cs-Alb-Dop] was evaluated using the MTT assay on a normal cell line. The results in Fig. 7 indicated that the system's cytotoxicity level never exceeded 20%, which means high degradability in normal cells. The color intensity in the assay plates further confirmed the biocompatibility of the system. Figure 7 illustrates the cytotoxicity results of the nanosystem and its components. The IC50 values for dopamine and the nanomanufacturing system indicated their relative safety in biological applications.

Hemocompatibility assessment of [Cs-Alb-Dop]

The hemocompatibility of the nanomanufactured system [Cs-Alb-Dop], along with its components, was evaluated to ensure its safety for potential in vivo applications, Fig. 7, also involved analyzing the hemolytic effects of each component, including dopamine, BSA, nano chitosan, and nanosystem [Cs-Alb-Dop]. The results indicated a concentration-dependent hemolysis. High hemolysis rates at certain concentrations could indicate potential cytotoxicity, a critical concern for clinical applications [31, 32, 34–42].

In summary, the hemocompatibility results form a crucial part of the preclinical safety assessment for the nanomanufactured system [Cs-Alb-Dop]. They not only demonstrate the system's potential impact on red blood cells but also highlight the pivotal role of concentration in determining its biocompatibility. These findings are instrumental in advancing the safe and effective application of this innovative nano manufactured system in therapeutic scenarios, particularly for the treatment of PD.

Conclusion

In this study, we have developed and analyzed an innovative nanomanufactured system [Cs-Alb-Dop], presenting a novel therapeutic approach to cross the BBB, a critical challenge in neurological therapies for PD. The incorporation of BSA into the platform not only improves the system's effectiveness in combating PD but also supports overall neural cell health. Our extensive analyses, including particle size (49.4 ± 9.9 nm), encapsulation

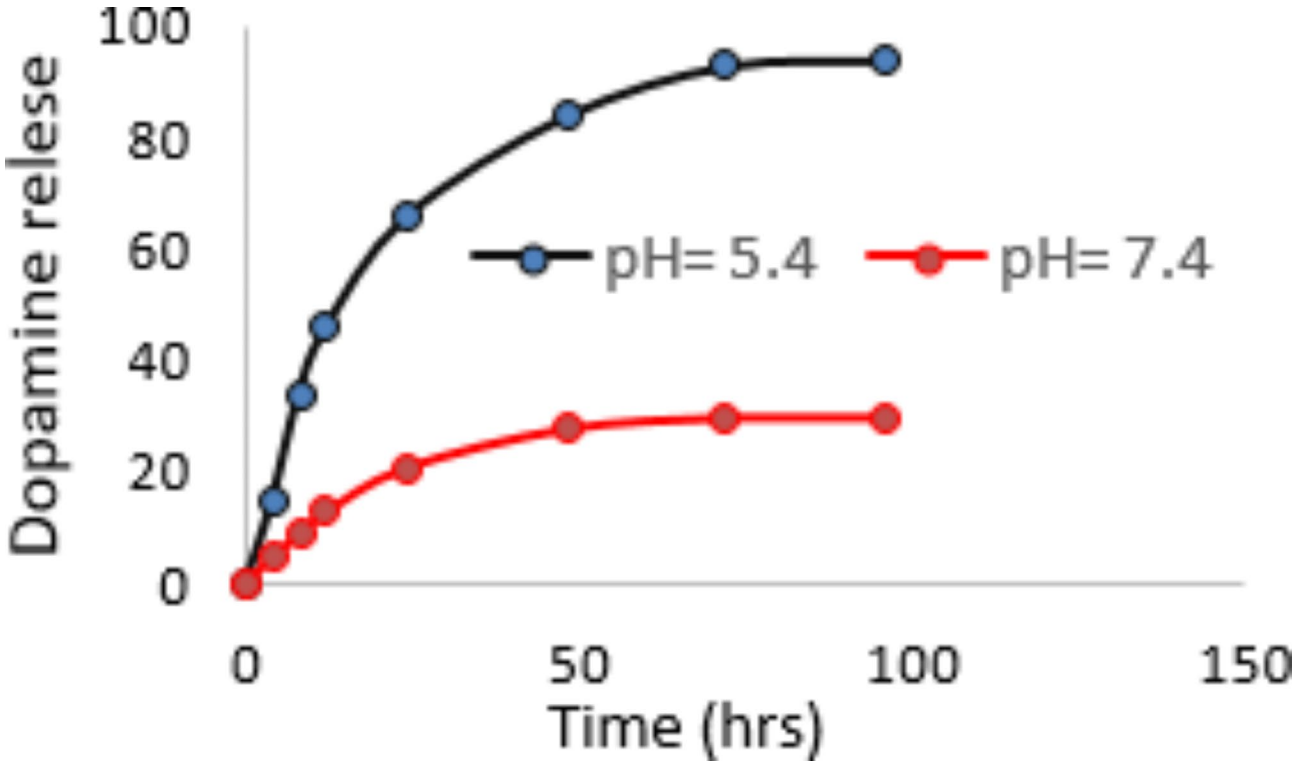

Fig. 6. Cumulative release of dopamine from nanosystem in pH 7.4 and pH 5.4.

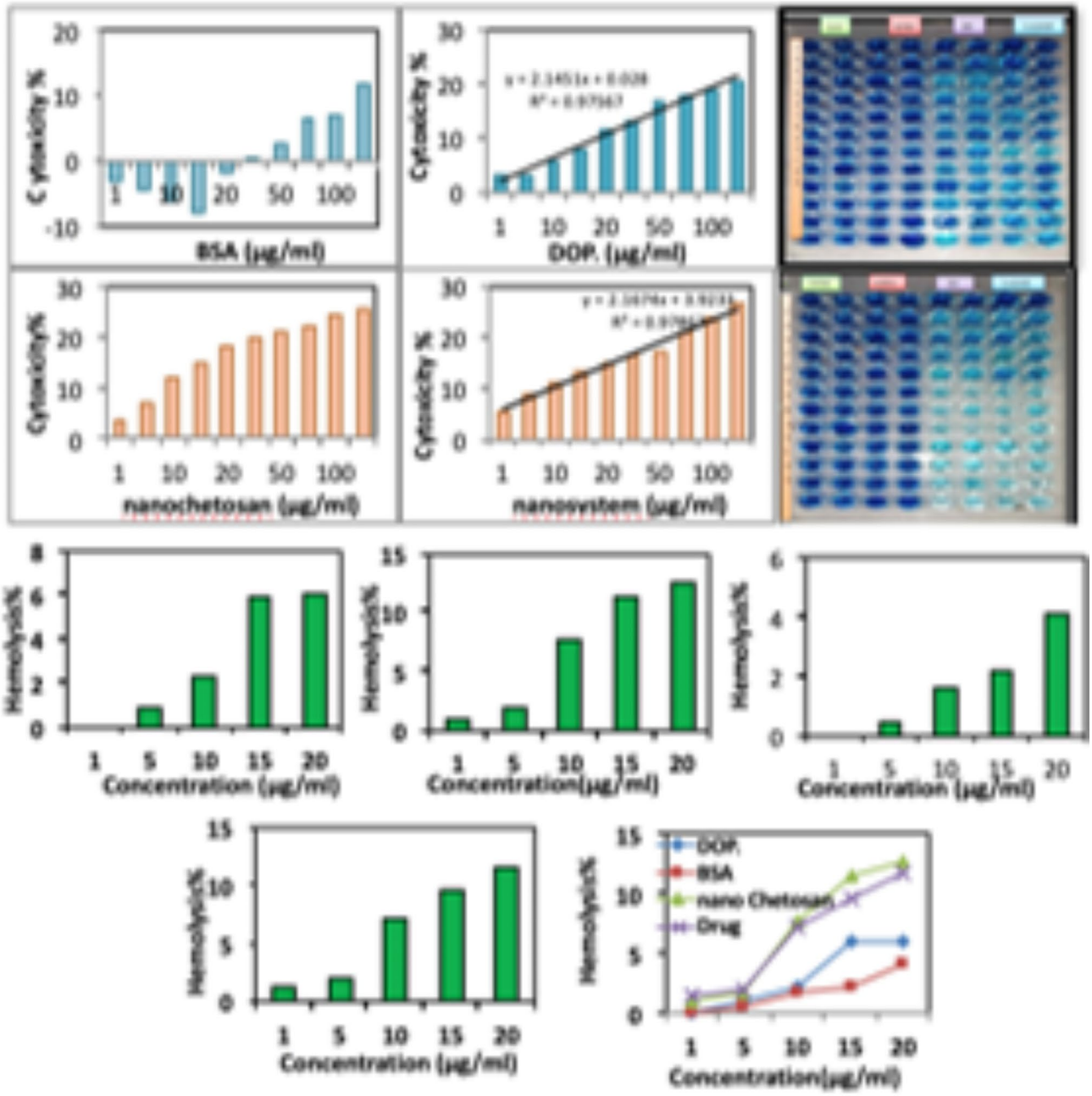

Fig. 7. Cytoxicity (IR) %. at 24 h and 48 h exposure time of each: (a) BSA. (b) Dop IC50=23.29 for 24 h exposure, and IC50 = 20.43 for 48 h exposure, (c) nanochitosan, IC 50= (d) [Cs-Alb-Dop], IC 50= 21.879 for 34 h exposure and IC50= 21. 25 for 48 h exposure.

efficiency (74.31 ± 0.29%), cytotoxicity (IC50 = 21.25), and hemocompatibility assessments (concentration-dependent), have confirmed the potential of [Cs-Alb-Dop]. We argue that the nanomanufactured system prepared here could be effective in treating PD and play a role in supporting cellular function and boosting body immunity,*in vivo* and *in vitro.* However, this nanosystem could cause renal dysfunction in animals if exceeds the dependent concentration, due to cytotoxicity by ROS or dopamine quinines. Therefore, Further studies are needed on lab animals to investigate the extent of ROS. We are also looking to improve dopamine release in the brain and liver and reduce the death of dopaminergic neurons. This system's potential applications extend beyond PD, suggesting its utility in the treatment of other neurological disorders and contributing to the broader field of neurotherapeutics.

Data availability

The authors declare that the data supporting the findings of this study are available within the paper and its Supplementary Information files.

Received: 28 June 2024; Accepted: 1 October 2024
Published online: 26 February 2025

References

1. -Smith, A. & Roberts, L. Exploring the use of nanocarriers for effective drug delivery in neurodegenerative diseases. *J. Nanobiotechnol.* **19** (1), 112 (2021).
2. -Johnson, K. & Patel, M. Nanotechnology in neurodegenerative disease: focus on Parkinson's. *Neurosci. Res.* **152**, 23–34 (2020).
3. -Lee, Y. & Kim, H. Advances in BBB crossing nanocarrier systems for drug delivery. *Eur. J. Pharm. Biopharm.* **142**, 55–70 (2019).
4. -Al-Obaidy, R., Haider, A. J., Al-Musawi, S. & Arsad, N. Targeted delivery of paclitaxel drug using polymer-coated magnetic nanoparticles for fibrosarcoma therapy: in vitro and in vivo studies. *Sci. Rep.* **13** (1), 3180 (2023).
5. -Gupta, S. & Kumar, P. Albumin-based nanoparticles in cancer therapy and imaging. *Bio Conjugate Chem.* **29** (6), 1823–1835 (2018).
6. -VeleshKolaei, M. R. H., Gill, P., Rafati, A. & Adiani, M. Bioinformatical Prediction of G-quadruplex Aptamer for detection of a Ligand in practice. *J. Appl. Sci. Nanatechnol.*, **3**(4). (2023).
7. -Davis, J. & Young, R. Chitosan-based systems for neuroprotective drug delivery: a review. *J. Biomedical Mater. Res. Part. A*. **110** (3), 865–878 (2022).
8. -AL-OGAIDI, A. J. M., Hamid, D. M. & Mohammed, A. A. R. Ultra Higher Assessment of CEA by using Sensing Technology. *Biochem. Cell. Archives*. **20** (2), 5307–5309 (2020).
9. -Sun, Q. et al. Preparation and characterization of chitosan microsphere loading bovine serum albumin. *J. Wuhan Univ. Technology-Mater Sci. Ed.* **27** (3), 459–464 (2012).
10. -Basosila, N. B. et al. Biogenic synthesis, Spectroscopic characterization and bioactivity of Cymbopogon citratus Derived Silver nanoparticles. *J. Appl. Sci. Nanatechnol.* **3** (4), 33–41 (2023).
11. -Robinson, F. & Lee, V. Nanomedicine for CNS disorders: opportunities and challenges. *CNS Drugs*. **34** (1), 9–23 (2020).
12. -Williams, L. & Brown, T. Nanotechnology in neurotherapeutics: a review. *Expert Opin. Drug Deliv.* **16** (6), 601–613 (2019).
13. -Khan, Z. & Singh, T. Overcoming the blood-brain barrier: nanoparticle-based therapies for neurological diseases. *Curr. Opin. Colloid Interface Sci.* **48**, 1–15 (2020).
14. -Edan, M. S. et al. *Effect of Silver Nanoparticles Synthesized by Pulsed Laser Ablation in Liquid on the Hematological, Hepatic, and Renal Functions of Albino rats* (Iraqi Journal of Science, 2023).
15. -Ortega, E. et al. Lipid nanoparticles for the transport of drugs like dopamine through the blood-brain barrier. *J. Nanopart. Res.* **23** (4), 106 (2021).
16. -Green, M. & Thompson, B. Albumin as a versatile platform for drug delivery: opportunities and challenges. *J. Controlled Release*. **285**, 57–70 (2018).
17. -Attallah, A. H., Abdulwahid, F. S., Ali, Y. A. & Haider, A. J. *Enhanced Characteristics of Iron Oxide Nanoparticles for Efficient Pollutant Degradation via Pulsed Laser Ablation in Liquid*1–14 (Plasmonics, 2024).
18. -Al-Jubori, A. A., Sulaiman, G. M. & Tawfeeq, A. T. Antioxidant activities of Resveratrol Loaded Poloxamer 407: an in Vitro and in vivo study. *J. Appl. Sci. Nanatechnol.* **1** (3), 1–12 (2021).
19. -Abdulwahid, F. S., Haider, A. J. & Al-Musawi, S. Folate decorated dextran-coated magnetic nanoparticles for targeted delivery of ellipticine in cervical cancer cells. *Adv. Nat. Sci. NanoSci. NanoTechnol.* **14** (1), 015001 (2023).
20. -Patel, S. & Johnson, J. Targeted nanoparticle systems for Parkinson's disease therapy. *Nanomed. Nanotechnol. Biol. Med.* **15** (1), 100–104 (2019).
21. -Robinson, D. & Lee, V. Nanotechnology in the treatment of neurodegenerative disorders: from concept to application. *Mol. Neurobiol.* **58** (4), 1735–1750 (2021).
22. -Williams, J. & Brown, T. Innovative approaches in nanomedicine for neurodegenerative disorders. *Neurotherapeutics*. **19** (2), 345–359 (2022).
23. -Abdulwahid, F. S., Haider, A. J. & Al-Musawi, S. Iron oxide nanoparticles (IONPs): synthesis, surface functionalization, and targeting drug delivery strategies: mini-review. *Nano*. **17** (11), 2230007 (2022).
24. -Aibani, N., Rai, R., Patel, P., Cuddihy, G. & Wasan, E. K. Chitosan nanoparticles at the biological interface: implications for drug delivery. *Pharmaceutics*. **13** (10), 1686 (2021).
25. -De Giglio, E., Trapani, A., Cafagna, D., Sabbatini, L. & Cometa, S. Dopamine-loaded chitosan nanoparticles: formulation and analytical characterization. *Anal. Bioanal. Chem.* **400**, 1997–2002 (2011).
26. -Attallah, A. H., Abdulwahid, F. S., Ali, Y. A. & Haider, A. J. Effect of liquid and laser parameters on fabrication of nanoparticles via pulsed laser ablation in liquid with their applications: a review. *Plasmonics*. **18** (4), 1307–1323 (2023).
27. -Barcia, E. et al. Nanotechnology-based drug delivery of ropinirole for Parkinson's disease. *Drug Deliv.* **24** (1), 1112–1123 (2017).
28. -Katas, H., Hussain, Z. & Awang, S. A. Bovine serum albumin-loaded chitosan/dextran nanoparticles: preparation and evaluation of ex vivo colloidal stability in serum. Journal of Nanomaterials, 2013, 1–9. (2013).
29. -Bronze-Uhle, E. S., Costa, B. C., Ximenes, V. F. & Lisboa-Filho, P. N. Synthetic nanoparticles of bovine serum albumin with entrapped salicylic acid. *Nanatechnol. Sci. Appl.*, 11–21. (2016).
30. -Solanki, R., Patel, K. & Patel, S. Bovine serum albumin nanoparticles for the efficient delivery of berberine: Preparation, characterization and in vitro biological studies. *Colloids Surf., a*. **608**, 125501 (2021).
31. -Al-Jubori, A. A. et al. Layer-by-layer nanoparticles of tamoxifen and resveratrol for dual drug delivery system and potential triple-negative breast cancer treatment. *Pharmaceutics*. **13** (7), 1098 (2021).
32. Trapani, A. et al. Characterization and evaluation of chitosan nanoparticles for dopamine brain delivery. *Int. J. Pharm.* **419** (1-2), 296–307 (2011).
33. Ragusa, A., Priore, P., Giudetti, A. M., Ciccarella, G., & Gaballo, A. (2018). Neuroprotective investigation of chitosan nanoparticles for dopamine delivery. Applied sciences, 8(4),474. Trapani, A., Mandracchia, D., Tripodo, G., Cometa, S., Cellamare, S., De Giglio, E.,… Antimisiaris, S. G. (2018). Protection of dopamine towards autoxidation reaction by encapsulation into non-coated-or chitosan-or thiolated chitosan-coated-liposomes.Colloids and Surfaces B: Biointerfaces, 170, 11–19.
34. Tang, S. et al. Brain-targeted intranasal delivery of dopamine with borneol and lactoferrin co-modified nanoparticles for treating Parkinson's disease. *Drug Deliv.* **26** (1), 700–707 (2019).
35. -Naskar, S., Sharma, S. & Kuotsu, K. Chitosan-based nanoparticles: an overview of biomedical applications and its preparation. *J. Drug Deliv. Sci. Technol.* **49**, 66–81 (2019).
36. Greco, I., Molchanova, N., Holmedal, E., Jenssen, H., Hummel, B. D., Watts, J. L.,… Svenson, J. (2020). Correlation between hemolytic activity, cytotoxicity and systemic in vivo toxicity of synthetic antimicrobial peptides. Scientific reports, 10(1), 13206.
37. -Burns, J., Buck, A. C., D'Souza, S., Dube, A. & Bardien, S. Nanophytomedicines as therapeutic agents for Parkinson's Disease. *ACS Omega*. **8** (45), 42045–42061 (2023).
38. Liu, Y., Luo, J., Liu, Y., Liu, W., Yu, G., Huang, Y., … Chen, T. (2022). Brain-targeted biomimetic nanodecoys with neuroprotective effects for precise therapy of Parkinson's disease. ACS Central Science, 8(9), 1336–1349.
39. -Weber, M. et al. Blood-contacting biomaterials: in vitro evaluation of the hemocompatibility. *Front. Bioeng. Biotechnol.* **6**, 99 (2018).
40. Shariare, M. H. et al. Phospholipid-based nano drug delivery system of curcumin using MSP1D1 protein and poloxamer 407: a comparative study for targeted drug delivery to the brain. *J. Nanopart. Res.* **26** (1), 12 (2024).

41. -Maghsoudnia, N., Eftekhari, R. B., Sohi, A. N., Zamzami, A. & Dorkoosh, F. A. Application of nano-based systems for drug delivery and targeting: a review. *J. Nanopart. Res.* **22**, 1–41 (2020).

Acknowledgements
The authors thank Mustansiriyah University, University of Technology and Saad Al-Witry neuroscience hospital for their support and help during data collection.

Author contributions
Aliaa has performed the experimental part, writing the first draft, editing, and authorizing the final draft. Zahraa designed the study, supervised the whole project, analyzed the data, Prepared and interrupted the results, participated in writing the first draft, revised, edited and approved the final version. Adawiya has participated in writing the first draft and the final version. Bahaa has consulted the neurological part of the study.

Funding
This project received no funds.

Declarations

Ethics approval and consent to participate
Written approval was obtained from the Ethical Approval Committee of the University of Mustansiriyah, Iraq. Study data/information was used for research purposes only. Informed consent was obtained from each participant. The HINARI (Health Inter Network Access to Research Initiative) programmer, established by WHO together with major publishers.

Competing interests
The authors declare no competing interests.

Additional information
Supplementary Information The online version contains supplementary material available at https://doi.org/10.1038/s41598-024-75116-7.

Correspondence and requests for materials should be addressed to Z.S.A.-G.